

Radiometric Calibration of the Hyperion Imaging Spectrometer Instrument From Primary Standards to End-to-End Calibration

Peter Jarecke and Karen Yokoyama

TRW Space and Electronics Group
Electro-Optical Systems and Technology Department

ABSTRACT

This paper describes the calibration transfer path from primary standards representing fundamental physical quantities through the calibration radiance source used in Hyperion instrument level absolute calibration. The calibration transfer path and hardware design of the primary and secondary standards and their validation for end-to-end calibration of the sensor are presented. The primary standards reside at the TRW Radiometric Scale Facility and include two high quantum efficiency Silicon photodiode trap detectors; an electrically self-calibrated pyroelectric detector serves as a secondary standard for cross-check. The end-to-end sensor calibration is accomplished with a Spectralon Panel Assembly source, that is illuminated by a NIST traceable FEL 1000 watt transfer standard lamp. An independent cross-check of the Spectralon reflectance properties is made with a transfer radiometer. An error analysis of the transfer path is presented. The basic strategy of the Hyperion end-to-end calibration is to reduce the length of the sensor responsivity error tree and to provide control of systematic errors as much as possible through cross-calibration.

1. INTRODUCTION

This paper presents the absolute radiometric calibration process and results of the Hyperion imaging spectrometer which operates from 0.4 to 2.5 microns. Hyperion will fly on the Earth-Orbiter 1 (EO-1) spacecraft for the New Millennium project (NMP). The New Millennium Program is an initiative to demonstrate advanced technologies and designs that show promise for dramatically reducing the cost and improving the quality of instruments and spacecraft for future space missions. Under this program, missions are intended primarily to validate such technologies and designs in flight by providing useful science data to the user community. The Earth Orbiter missions will validate by space flight, advanced technologies for the next generation Earth Science Systems Program Office science needs. The other payloads on the spacecraft are the Advanced Land Imager (ALI) and Atmospheric Corrector (AC). The payloads have been integrated onto the spacecraft at Goddard Space Flight Center and launch is currently scheduled late in the year 2000. The Hyperion sensor design and radiometric performance is described in an accompanying paper titled "Radiometric Performance Characterization of the Hyperion Imaging Spectrometer Instrument".

An absolute radiometric irradiance scale has been realized at TRW consisting of two high quantum efficiency Silicon photodiode trap detectors, NIST traceable FEL 1000 watt lamps, and an electrically calibrated pyroelectric detector. The scale covers from 0.4 to 2.5 micrometers in wavelength and from 20 to 200 watts/m²-μm irradiance which is sufficient to cover the dynamic range of the Hyperion sensor. A secondary standard radiance source is created to calibrate the Hyperion sensor end-to-end. This radiance source consists of the FEL 1000 watt lamp illuminating a 0.25 meter square Spectralon plate from a distance of 0.50 meters an angle normal to the plate. The lamp and plate are mounted on a structure and called the Spectralon Panel Assembly (SPA). This structure is mounted to the vacuum chamber where its illumination fully fills the Hyperion sensor field of view and entrance aperture by passing through a fused silica, SiO₂ window.

A cross-calibration of the radiance from the panel is made using a transfer radiometer with one of the Silicon photodiode trap detectors. The aperture area-field of view product ($A\Omega$) is calculated independently from component parts. The basic strategy of the Hyperion end-to-end calibration is to create an absolute primary scale close to the assembly and test facilities and make the train from primary standard short and cross-calibrated. This plan is designed to reduce the length of the sensor responsivity error tree and provide control of systematic errors.

2. PRIMARY IRRADIANCE SCALE

The source of radiant power for realizing an irradiance scale at TRW is the Sylvania FEL 1000 watt Quartz Tungsten Halogen (QTH) lamp. Four lamps (part number OL FEL-C) were purchased from Optronics Inc. Two (SN F-543 and SN F-544) were calibrated by Optronics Laboratories, Inc. relative to the same type of lamp which Optronics procured from the National Institute of Standards and Technology (NIST). The calibration of the lamp from NIST is calibrated by a procedure defined in NIST a special publication, Standard Irradiance Calibrations No.250-20 Sept. 1987 (Ref 1).

To cross-calibrate these lamps, three detector based irradiance standards are employed each fitted with a different precision entrance aperture. Two of the standards are based on the high quantum efficiency (HQE) photodiode trap detector Ref(2), Ref(3) and Ref(4). The two independent HQE trap detectors are a UDT (Graseby) QED-150 which uses three EG&G UV444B Si detectors and a (SPR-73), which is supplied by Cambridge Instrumentation and Research, Inc (CRI). The SPR-73 uses three windowless Hamamatsu S1337-1010 detectors.. The third primary detector standard used here is the LaserProbe Inc. RS-5900 SN 9409-035 electrically calibrated pyroelectric radiometer (ECPR). This absolute self-calibration technology was developed by Doyle, McIntosh (Laser Precision Corp) and Geist (NIST) (Ref 5).

An HQE trap Si photodiode primary standard detector using Hamamatsu photodiodes has been cross-calibrated with a helium cooled active cavity radiometer primary standard at CRI and agreement of 0.02 % was achieved (Ref 6). While the systematic error of the ECPR, estimated at about 1% (Ref 5), is much greater than the Si trap detector error, it serves two purposes for the Hyperion calibration. First, it is a crosscheck to rule out large errors in the use of the HQE trap Si photodiodes. Secondly, it serves to extrapolate the calibration from the 0.9 micron wavelength cutoff of the Si trap detector out to 2.5 micron cutoff of the Hyperion HgCdTe SWIR focal plane array.

Effective Wavelength	Effective Bandwidth	Effective Wavelength	Effective Bandwidth
[microns]	[microns]	[microns]	[microns]
402.3	2.41	999.9	5.69
450.9	5.66	1052.5	5.72
502.2	6.50	1099.5	4.42
549.4	4.16	1199.6	3.16
601.6	5.92	1298.6	4.08
651.6	6.74	1388.3	3.05
698.4	5.29	1499.7	4.02
751.9	5.24	1552.7	6.75
800.5	5.61	1600.8	5.30
901.7	7.74	1648.2	4.86
		1701.1	4.68
		1794.1	5.19
		1899.8	6.15
		1999.6	6.58
		2095.8	4.87
		2193.1	2.85
		2297.0	5.51
		2400.2	7.51
		2498.1	3.74

Table 1. Effective Wavelengths and Bandwidths of the Narrowband Filters

The source of irradiance for the scale is the FEL 1000 watt lamp. Comparisons of the three primary standards were made to realize an irradiance scale for Hyperion. First, the two trap detectors' spectral responsivity was compared using a HeNe laser line source, which under filled each entrance aperture (so the comparison was in radiant power). The signal was varied using a polarizer over the dynamic range from 1 to 60 microwatts and the agreement was $0.080 \% \pm 0.033 \% 1\sigma$ using

linear regression over 12 signal levels. When the same comparison was made between the QED-150 and the LaserProbe ECPR an agreement in response to the HeNe laser line source of $0.34 \% \pm 0.014 \%$ was obtained from the linear regression.

Spectral irradiance levels were measured at the wavelengths defined by a set of 10 narrowband filters in the visible region listed in Table 1. The filter bandpasses were measured with a Cary 5 spectrometer and the linearity was checked a HeNe laser at $0.6328 \mu\text{m}$ using the SPR-73 trap detector as a reference. The precisely determined entrance apertures of the three detectors are 0.202 cm^2 (SPR-73), 0.0803 cm^2 (QED-150) and 0.50 cm^2 (ECPD). The lamp is set at 0.50 meters from each of the precision detector entrance apertures using a metering rod. The lamp filament alignment is adjusted with a jig, which reproduces the precise original orientation of the filament at the time of calibration relative to a given aperture in front of a detector illuminated by the lamp. A linear regression of the responses between the QED-150 and the LaserProbe ECPR to the lamp irradiance in 9 of the bands produced an agreement in relative response of $0.68 \% \pm 0.88 \% 1\sigma$. The dynamic range for the regression is set by the change in lamp irradiance from 0.4 to 0.9 microns in the narrowbands. A second linear regression of the responses of the QED-150 and SPR-73 in 8 of the bands (one was being replaced at the time) produced an agreement in response of $0.34 \% \pm 0.76 \%$.

Using the absolute irradiance measurements of the lamp at 0.50 meters in the 10 wavebands from 0.4 to 0.9 microns and measurements made with the ECPR in another 19 wavebands from 1.0 to 2.5 microns (see Table 1), an absolute spectral irradiance curve for the lamp is generated and shown in Figure 1. The curve fit through the points is a graybody with temperature of 3100 Kelvins and an emittance which is smoothly and monotonically decreasing by 35 % over the wavelength range. The RMS variation of the points about the curve fit is 0.97 % if four of the bands are not included. These four bands were high by $> 3\sigma$ and this may have been caused by residual, uncorrected out-of-band response. Spectral irradiance for all bands is plotted in Figure 1. The Optronics calibration delivered with the lamps is shown as gray circles. The deviation between the Optronics calibration and the TRW measurement is shown in Figure 2.

3. THE SECONDARY RADIANCE STANDARD SOURCE

To create a secondary standard source of radiance, which fills the full aperture, and field of the Hyperion sensor, an assembly is used to hold the FEL lamp in its adjustable set of stages at a distance of 0.50 meters from a $0.25 \text{ meter square}$ plate of Spectralon. The lamp illuminates the plate at a normal angle and the assembly is mounted on the door of the vacuum chamber used for radiometric testing of the sensor. The sensor views the plate from inside the chamber through an uncoated SiO_2 window. A wall in the assembly prevents direct view of the window by the lamp, which is gold plated on the lamp side for thermal control, as the 1000 watt lamp is very hot. The geometry is shown in a drawing in Figure 3 and the Spectralon Plate Assembly (SPA) is shown mounted to the wall of the chamber in the photo in Figure 4.

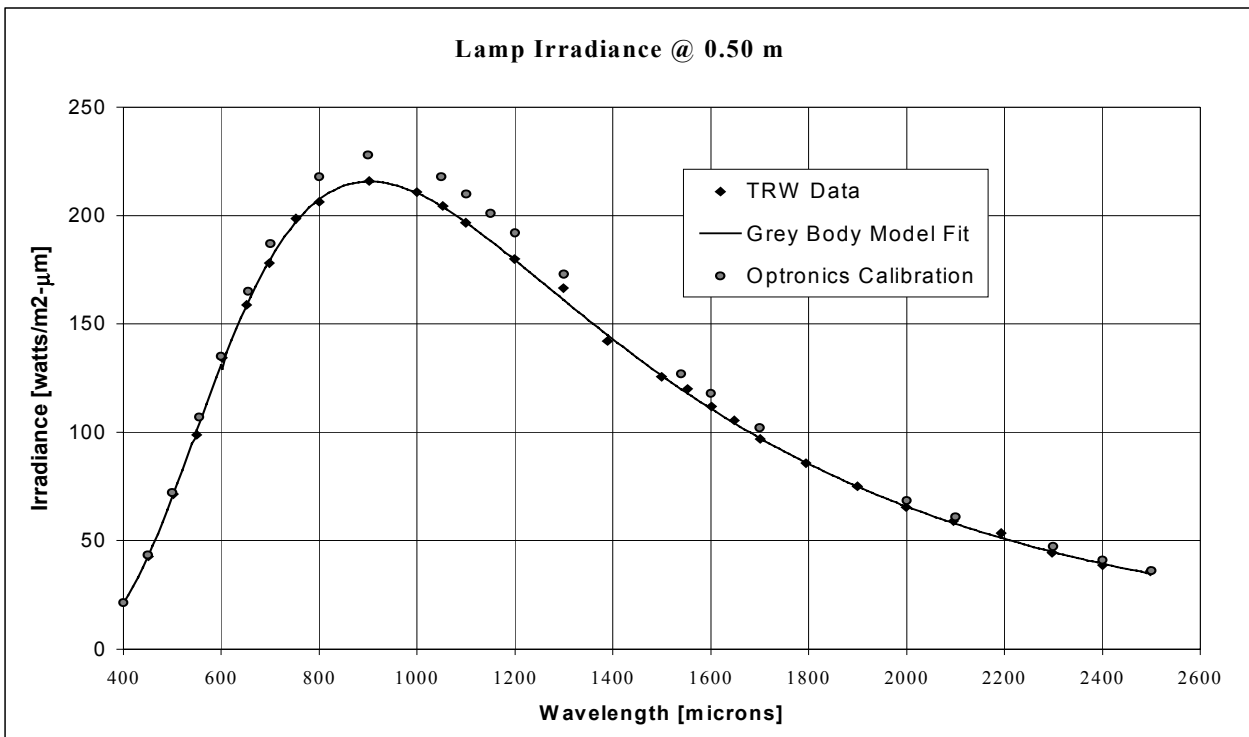


Figure 1. Spectral Irradiance of the FEL Lamp (SN 543 Measured With the Primary Standard Detectors)

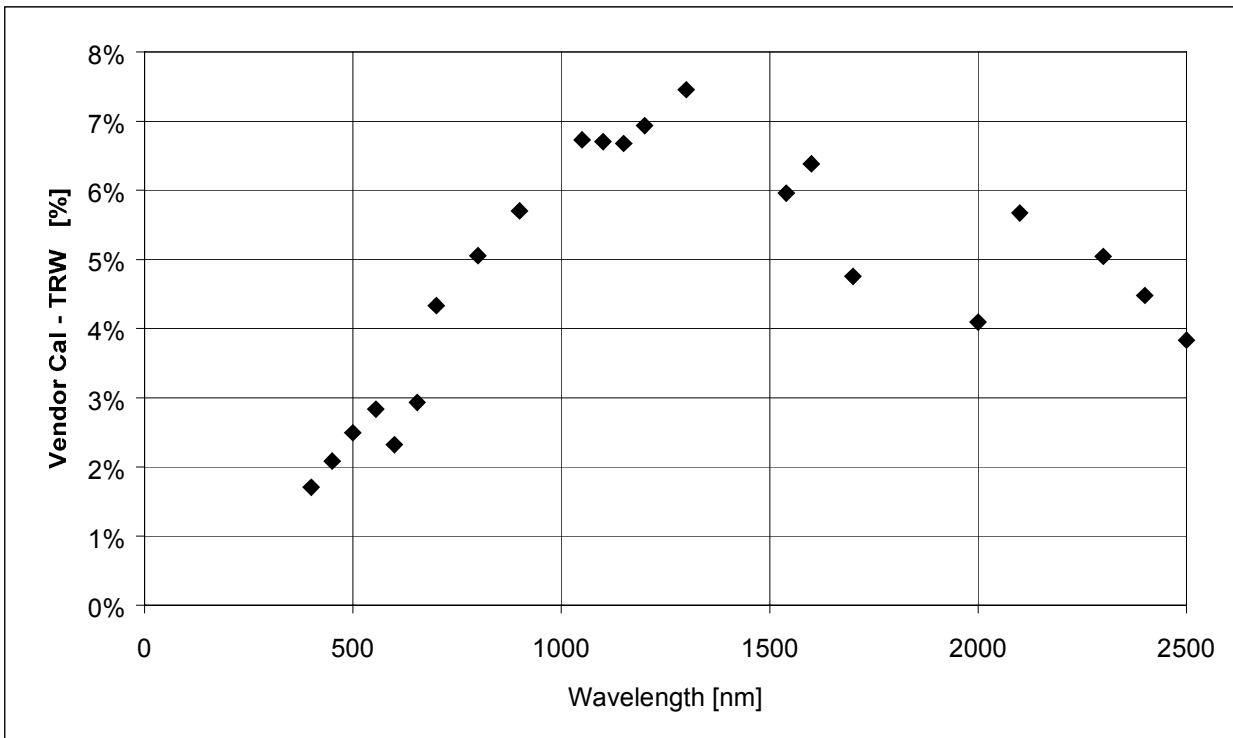


Figure 2. The vendor lamp calibration values are from 2 % to 7 % higher that the TRW Si Photodiode Priamry Standard.

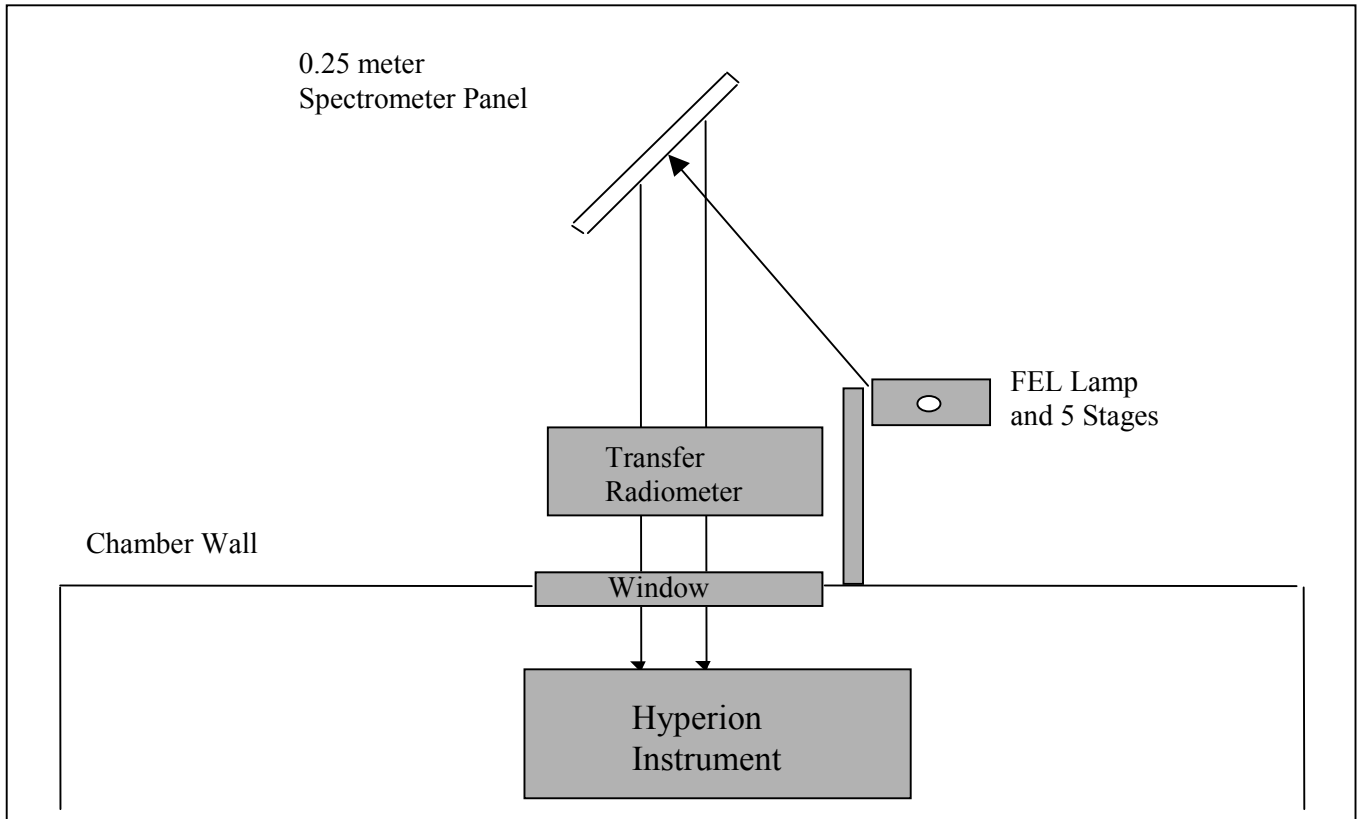


Figure 3. Schematic of the Layout of the Spectralon Panel Assembly Mounted on the Chamber Wall

To first order, the radiance from the Spectralon plane is the irradiance divided by π if the BRDF of the panel is perfectly Lambertian. It is critical to know the BRDF and reflectance of the plate over the angles and spatial extent viewed by the sensor. Reflectance properties of the Spectralon plate are taken from vendor specifications and measurements made at TRW with the Optical Scatter and Contamination Effects Facility. The Hyperion sensor full field of view is 0.45 degrees and the entrance aperture is 0.125 meters. The sensor views the Spectralon plate at a distance of about 1 meter at an angle of incidence of 26 degrees.

The lamp filament at 0.5 meters distance from the normal to the plate varies in distance from the plate over the extent of the view or footprint of the sensor on the plate. This results in a ± 7 degree variation in angle of incidence; hence, a rolloff of irradiance on the plate occurs, which varies as the function \cos^3 of the angle of incidence. A \cos^4 law is not expected because the shape of the filament is a vertical cylinder. This rolloff becomes as large as 2.5 % at the edges of the sensor view of the plate and the weighted mean reduction in irradiance from the normal or nadir view is 1.0 %.

This rolloff was confirmed by using an ASD Field Spec spectral radiometer. The radiometer used at 5 degrees FOV was placed viewing the panel at an angle of incidence of 26 degrees which is identical to the Hyperion view. The footprint on the panel is about 20 % of the Hyperion footprint. The ASD was translated from left to right to move its FOV across the Hyperion footprint and data were taken at five locations covering the full diameter. The 2.5 % rolloff was confirmed to within a precision of 20 %.

As a cross-check of the assumed properties of the Spectralon used to convert irradiance to radiance, a transfer radiometer is employed as shown in Figure 3 which uses an off-axis parabola mirror and a fold mirror with a precision entrance aperture of 2.22 cm and the SRF-73 trap detector. A 0.7 to 0.9 micron bandpass filter limits the spectral range. The increased spectral bandwidth is necessary to allow adequate signal at the reduced values produced by the radiance from the Spectralon plate. This radiometer is placed in the SPA at about 0.5 meters from the plate in a position to view the plate along the same line of sight as the Hyperion sensor. The transfer radiometer rests in this position outside of the SiO₂ window of the vacuum chamber.

Data are taken with the transfer radiometer in three configurations: 1) with the lamp and plate alone without any assembly structure in place; 2) with the SPA fully assembled; and 3) with the SPA mounted on the vacuum chamber wall. The expected signal from the trap detector in the transfer radiometer is calculated, in advance, using the measured lamp irradiance, the reflectance properties of the Spectralon and the throughput of the transfer radiometer. The throughput is determined from the A Ω of the transfer radiometer, which is calculated from precision measurements of the aperture areas and the focal length of the off-axis parabola (OAP) in the radiometer. The transmittance of the 0.7 to 0.9 μm bandpass and the reflectances of the protected silver coated OAP mirror and fold mirror are included in the calculation. This calculated value is compared in Table 2 below with four measurements taken in the three configurations listed above

The radiance from the SPA, which is mounted on the chamber wall, is used to absolutely calibrate the Hyperion sensor. This radiance is corrected for the \cos^3 profile described above and the transmittance of the uncoated SiO₂ vacuum chamber window. The vacuum chamber wall on which the SPA is mounted is painted white. A black painted sheet of Aluminum is hung on the wall to reduce the light from the lamp that is scattered back to the SPA panel. Measurements of this scatter radiance from the black sheet were made with the the ASD Field Spec spectral radiometer. Illumination from this source produces less than 0.1 % increase in radiance of that from direct illumination by the lamp. The SiO₂ window also reflects back to the panel with a reflectance of about 4 % per surface. A calculation of the expected return to the SPA panel from this source is also about 0.1 %. This reduction is produced radiometrically by the ratio of the apparent solid angle of the panel (as it views its own reflection) to the solid angle, π , into which the 8 % contribution is re-scattered.

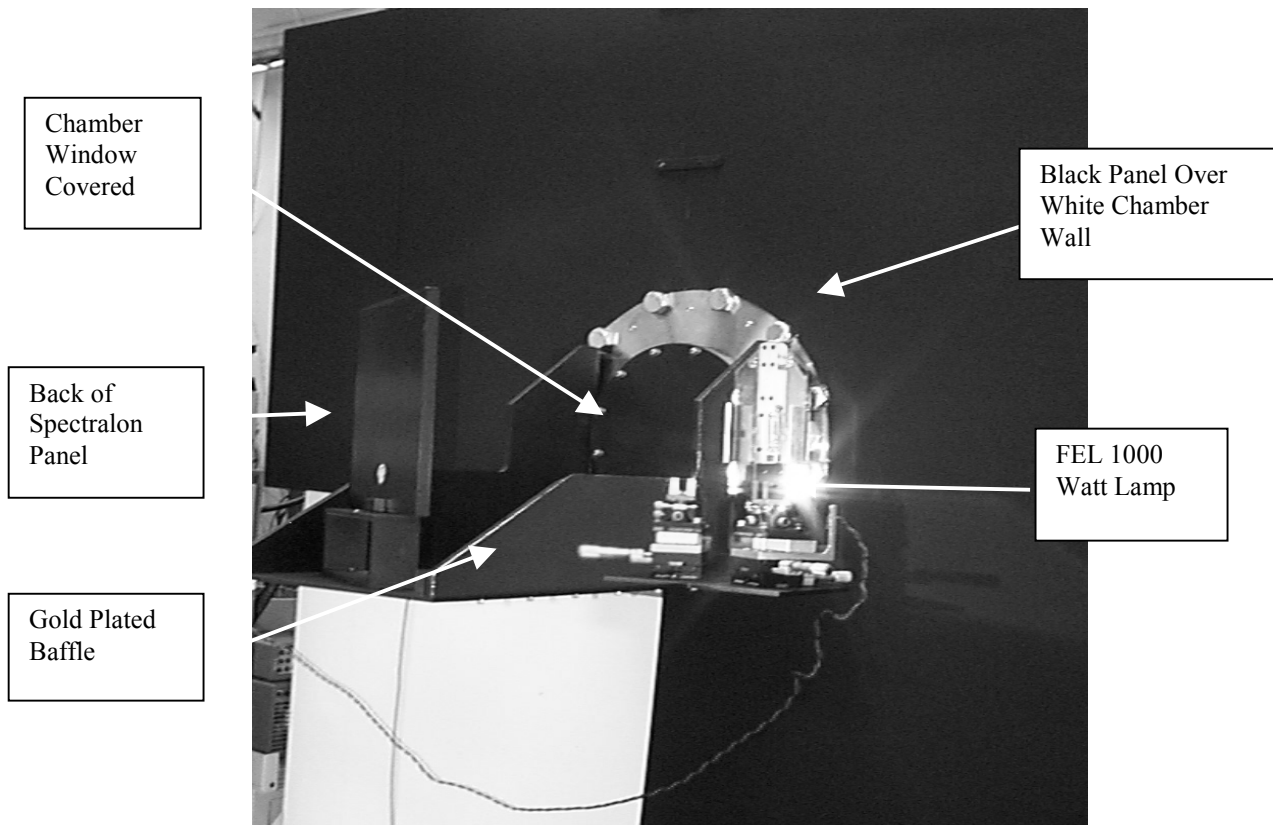


Figure 4. Photo of the SPA Mounted on the Vacuum Chamber Wall with the FEL 1000 Watt Lamp Powered.

Date	Configuration	Lamp Age [Hours]	Expected Signal [μA]	Measured Signal [μA]	Relative Difference [%]
5/6/99	Panel on open bench	25.4	0.3487	0.3502	0.41
5/6/99	Panel mounted in assembly on bench	30.1	0.3487	0.3527	1.13
6/8/99	Panel assembly mounted on Vacuum chamber	39.4	0.3487	0.3505	0.51
7/2/99	Panel assembly mounted on Vacuum chamber	68.6	0.3487	0.3509	0.61

Table 2. Agreement Between Measured and Calculated Transfer Radiometer Radiance Values for the SPA.



4. Error Budget and Conclusions

The results in Table 2 suggest that the radiance scale produced by calculating the expected conversion from irradiance of the lamp at the Spectralon plate to radiance using the assumed properties of reflectance and scatter characteristics the plate is consistent with the optical throughput of the transfer radiometer at about the 0.8 % difference level (RMS of Table 2 results). To determine the expected agreement between these two radiance determinations, an error budget for the two conversion processes described in sections 2 and 3 is made based on the steps in the processes and presented in Table 3a and 3b. All error estimates in the tables are 1 σ and combined by RSS.

It would appear that the predicted errors in comparison of the two conversions of the irradiance on the SPA to radiance are larger than the measurements in Table 2. Perhaps two of the larger error terms were in the same direction and cancelled out. We conclude from the results in Tables 2 and 3 that the conversion has a probable error on the order of 1% using both methods as a self-consistency check. Table 4 shows the error budget estimate for the lamp irradiance measurement and Table 5 estimates the entire SPA radiance source error. Note that the same detector is used for both the lamp irradiance measurements and the transfer radiometer.

A primary irradiance scale is realized at TRW with agreement between absolute detector standards better than 1 %. This scale is used to create a secondary radiance scale using a Spectralon Panel. The predicted radiance accuracy is better than 2 %. This is based on the agreement between the cross comparison of two different ways of determining the irradiance to radiance conversion. One used validated relative BRDF properties of Spectralon and vendor data for absolute reflectance. The other used a transfer radiometer with an independently determined $A\Omega$. This Spectralon panel radiance source was used to calibrate the Hyperion sensor.

Error Term	Error [%]
Reflectance at 26° Angle of Incidence	1.0
Scatter Uniformity with Angle	0.5
Stray Light	0.2
Total Error	1.35

Figure 3a. Conversion from Irradiance to Radiance Using Spectralon Scatter Properties

Error Term	Error [%]
Entrance Aperture Area	0.5
Field Stop Area	0.2
OAP Focal Length	0.4
$A\Omega$ Calculation	0.3

Figure 3b. Direct Measurement of Radiance with Calculation of $A\Omega$ for the Transfer Radiometer

Lamp Irradiance	Error [%]
Primary Standards	0.29
Agreement	0.1
Trap Detector Ammeter Calibration	0.3
HQE Correction	0.1
Lamp-Trap Detector Distance	0.5
Precision Aperture Area	0.5
Filament Alignment Repeatability	0.3
Lamp Current Repeatability	0.1
Filter Effective Bandwidth	1.0
Interpolation Between Band Data Points	0.5
Total Lamp Irradiance Subtotal	1.39
Conversion to Radiance	1.0
Stray Light Contamination	0.5
SiO ₂ Window Transmittance	0.5
Total Error	1.85

Figure 4. Error Estimates for Lamp Spectral Irradiance Which is Given as a Sub-total and Total SPA Radiance Below. Errors are 1 σ RMS.

5. Acknowledgements

The authors wish to acknowledge the support of the NASA Goddard Space Flight Center for their support on the Hyperion Program Contract No. NAS5-98161. We also acknowledge the helpful discussions and manufacturing support of our TRW colleague, Steve Lai.

6. References

1. J. H. Walker, R. D. Saunders, J. K. Jackson, D.A. McSparron, "Standard Irradiance Calibrations", NBS Special Publication No.250-20 (1987)
2. J. Geist, "Quantum Efficiency of the p-n Junction in Silicon as an Absolute Radiometric Standard.", Appl. Opt. **18**, 760 (1979)
3. J. Geist, E.F. Zalewski and A.R. Schaefer, "Spectral Response Self-Calibration and Interpolation and Silicon Photodiodes", Appl. Opt., **19**, 3795 (1980)
4. N. P. Fox, "Trap Detectors and Their Properties", Metrologia, **28**, 197 (1991)
5. W. M. Doyle, B. C. McIntosh and J. Geist, "Implementation of a System of Optical Calibration Based on Pyroelectric Radiometry", Optical Eng., **15**, 541, (1976)
6. E. F. Zalewski and C. C. Hoyt, "Comparison Between Cryogenic Radiometry and the Predicted Quantum Efficiency of pn Silicon Photodiode Light Traps", Metrologia, **28**, 203, (1991)